

Driving Using Model Predictive Control

Technical Report on Automatic Control
vol. TRAC 3, December 2008, available online at: www.rt.mw.tum.de.

Zongru Yang, Boris Lohmann

Abstract—Driving as an incremental forming method can create almost any 2D and 3D sheet metal parts using universal tool sets. In this paper, stretching as an approach of the driving is modelled through the three phases that are the hybrid deformations, the material flows and the springback. In comparison with the experiment results, the stretching model is acceptable to be employed in the model predictive control that can supply the optimal control input through minimizing the objective function. The optimization problem is solved by the use of the discrete dynamic programming. The optimal control input results from the optimal path with minimal costs. The according parameters that can affect the control output are tuned to find out a reasonable combination of them that yields rational control outputs.

I. INTRODUCTION

Driving is one of the oldest manufacturing methods. It allows the creation of nearly any two or three dimensional geometry using universal tool sets [1], which satisfies different customer demands for product individualization [2].

Driving is an incremental forming process carried out by relatively small, inexpensive C-frame presses. It has a high degree of the interaction between tools and materials, in which material properties are changed by work hardening and where contact conditions are varied with every forming stroke. After a multitude of strokes the shapes of work pieces suffer from accumulated inaccuracies. In order to automate this process, a sensor system was employed to get feedback of state deformations of the work pieces [3][4]. Using a fuzzy controller and a switching P-controller respectively, the driving loop was closed to shape the sheet metal parts in the desired forms. These two control strategies can be easily implemented. But it is time-consuming to tune them for just suiting the changing of the state parameters. Sometimes the tuning could be unachievable. At this point, *Model Predictive Control* (MPC) as a new control strategy is proposed to suit for changing of system parameters and making the end forms precisely.

Nowadays, MPC is a popular control strategy and widely used in the process industry [5]. It uses a model of processes to get a control law by minimizing an objective function. It is a totally open methodology based on certain basic principles.

In section 2, the driving process will be modeled. Using this model, the strategy, the algorithm and the results of

MPC will be presented in section 3. The section 4 will give conclusions and future works.

II. MODELING

Using the driving machine, the L-shaped metal sheets can be stretched or shrunk in processes by means of hammering strokes on the metal sheets. During every forming stroke, the tools clamp the sheet and transform the vertical stroke into horizontal movement and by that induce compressive (shrinking) or tensile (stretching) stress into the sheet. So the sheet can be bended at different positions into a given 2D form. The forming force can be applied manually or automatically by tuning the stroke depth, which denotes the distance between the upper and the lower tool part. In the paper, only the stretching process will be modeled.

A. Geometry Approximation of L-Shaped Metal Sheets



Fig. 1. L-sheet with a bending angle at the stroke position

In Fig. 1, the L-sheet was stretched in the middle resulted with a certain angle. It is seen that the L-sheet has the two flanks and the transition zone between the both. In the forming process, the material of the upper flank is extended in the plain at the stroke position but in different rates. The nearer the stroke points are located at the transition zone, the less the material is elongated. The lower flank is orthogonal to the upper flank and is therefore only bended through the forming force of the upper flank. In order to make the analytical modeling of the stretching process possible, it is necessary to approximate the geometry of the L-sheet. For the approximation, it is assumed that the length of the L-sheet stays constantly. Hence, the L-sheet can be seen as the combination of the two flanks that have a common edge with a constant length and the transition zone is replaced with constraints. Fig. 3 shows the deformations of the two flanks after some strokes. The two flanks are constrained at

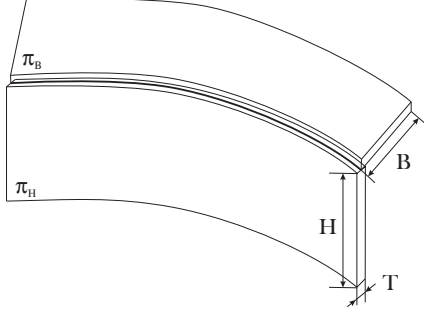


Fig. 2. Approximated geometry model of the L-sheet (1).

the fiber with the constant length l_0 . In the flank π_B , the major strain ϵ_{1B} is calculated as follows:

$$\epsilon_{1B} = \int_{l_0}^{l_B} \frac{dl}{l} = \ln \left(\frac{l_B}{l_0} \right). \quad (1)$$

With the equations $l_B = \theta(\rho_B + y_B)$ and

$$l_0 = \theta\rho_B \quad (2)$$

, the strain ϵ_{1B} is gained at the position y_B :

$$\epsilon_{1B} = \ln \left(1 + \frac{y_B}{\rho} \right) \approx \frac{y_B}{\rho}. \quad (3)$$

Identically, the major strain ϵ_{1H} in the part π_H is y_H/ρ .

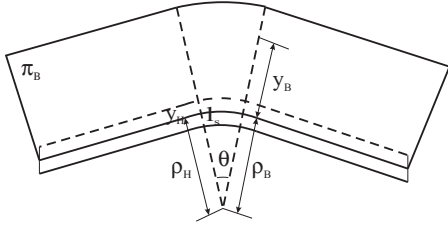


Fig. 3. Parameterization of the bended L-sheet for calculating strains. This is the topview of the approximated geometry model (2).

B. Process of Sheet Metal Deformations

By a hammering stroke, the upper tool moves downwards to the upper surface of the L-sheet and brings the force into the L-sheet successively. There are three phases in this total process. In the first phase, the two flanks π_B , π_H will be formed till the flow limit of the material. The second phase indicates the material flow procedure that happens simultaneously in both flanks. With the decreased force on the L-sheet, the two flanks spring back in the third phase, which can also cause the reverse bending. In the following, these three phases will be detailed described.

1) *Hybrid Deformations of L-Sheets*: In this phase, there exist two forming steps that denote the hybrid deformations of the two flanks π_B , π_H [6]. At the first step, the two flanks are formed only elastically. The Hookes's law yield the stress-strain relation in the material $\sigma_1 = \bar{E}\epsilon_1$ ($\bar{E} = E/(1-\nu)$), that is to say, the stress increases proportionally with the forming rates. If the stress exceeds the elastic limit, the material goes into the plastic or flow phase. Hereby, a

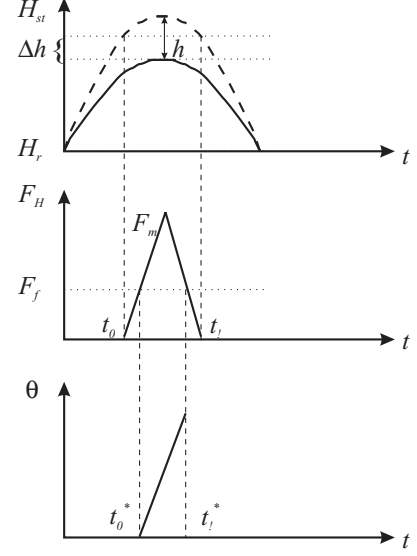


Fig. 4. Phases of deformations of the L-sheet at one stroke in stretching processes. The time responses of the movements of the upper tool (top), the forces on the surface of the L-sheet (middle) and the bending angle (bottom).

simple material model is used to interpret the adjoined two steps. It has an elastic or a proportional part and a perfect plastic part. At the second step, the flank π_B stays elastically, while the flank π_H goes into the flow. The major stress σ_{1H} in the flank π_H has a constant flow stress S_H . Till $\sigma_{1B} = S_B$, the flank π_B begins to flow. After these two steps, the L-sheet has been already formed in the small angle θ [6]:

$$\theta = \frac{2S_H l_0}{\bar{E}T}. \quad (4)$$

The force limit F_f can be calculated in the following [6]:

$$F_f = \frac{1}{4}(2BS_B + HTS_H/B). \quad (5)$$

If the horizontal force on the surface of the L-sheet is greater than F_f , the forming process goes into the second phase.

2) *Procedure of Material Flows*: Although the L-sheet is totally in the flow phase, the flank π_H is formed only passively and can be ignored because of its small deformation energy. But it must exist for keeping the constraints to continue the forming of the flank π_B . The figure 5 shows

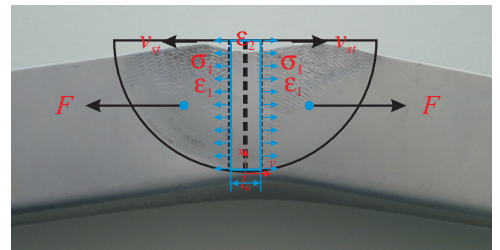


Fig. 5. Flat strain-stress states on the L-sheet under the horizontal velocity of the tool V_{st}

the plane stress on the flank π_B :

$$\begin{aligned} \epsilon_1; \quad \epsilon_2 = -\epsilon_1; \quad \epsilon_3 = 0; \\ \sigma_1; \quad \sigma_2 = 0; \quad \sigma_3 = 0; \end{aligned} \quad (6)$$

with the constraints

$$\epsilon_1|_{y=0} = 0; \quad \dot{\epsilon}_1|_{y=0} = 0, \quad (7)$$

where $\dot{\epsilon}_1$ is the velocity of the deformation that is defined by the velocity of the displacement v_1

$$\dot{\epsilon}_1 = \frac{\partial v_1}{\partial x}. \quad (8)$$

The velocity of the displacement can be evaluated through the velocity of the tool in the horizontal direction V_{st}

$$v_1 = \frac{2V_{st}}{Bl_0}xy. \quad (9)$$

Hereby, the velocity V_{st} is approximated by

$$V_{st} = \frac{1}{2} \frac{\partial H_{st}}{\partial t} \Big|_{t=t_0^*}, \quad (10)$$

and it stays constant in the flow time interval. Altogether, the velocity of the deformation $\dot{\epsilon}_1$ is calculated as follows:

$$\dot{\epsilon}_1 = \frac{2V_{st}}{Bl_0}y. \quad (11)$$

In order to gain the bending angle, the strain at the boundary of the flank π_B is determined in a time interval Δt

$$\epsilon|_{y=B} = \int_0^{\Delta t} \dot{\epsilon}|_{y=B} d\tau = \dot{\epsilon}|_{y=B} \Delta t. \quad (12)$$

It should be denoted that the velocity of the deformation keeps constant in the time interval Δt . The figure 4 shows the time response of the upper tool movement $H_{st}(t)$, the force on sheets $F_H(t)$ and the bending angle $\theta(t)$. Along the response till the time t_0 , the upper tool contacts the surface of the sheet. At the time point t_0 , the slackness between the sheet and the tool is removed and the lower tool does not slacken any more. Since this time point

$$t_0 = \frac{1}{\omega} \arcsin \left(\frac{A_{st} + \Delta h}{A_{st} + h} \right), \quad (13)$$

the force on the sheet rises linearly to the maximum F_m and then falls off. Hereby, Δh indicates the slackness between the upper tool and the sheet and the slacked offset of the lower tool. It is formulated as follows:

$$\Delta h = \xi \frac{\bar{H} + \bar{h}}{H_r + \bar{h}} h, \quad (14)$$

where ξ is the transfer factor that describe the effect of the initial movements of the tools in vertical and horizontal directions, in which the slackness disappears and the tools don't slide on the surfaces any more. The reference distance $\bar{H} + \bar{h}$ is brought in the calculation because the tool moves itself from a reference position. The value \bar{H} and \bar{h} can be arbitrarily chosen in the valid intervals with suitable ξ . Since the time point

$$t_1 = \frac{1}{\omega} \left[\pi - \arcsin \left(\frac{A_{st} + \Delta h}{A_{st} + h} \right) \right], \quad (15)$$

the upper tool leaves from the surface. In the time interval $[t_0^*, t_1^*]$, the material flows when the force F_H on the surface of the L-sheet exceeds the limit F_f (Eq. 5) and

$$t_0^* = \frac{F_f}{2\eta F_m} (t_1 - t_0) + t_0, \quad (16)$$

$$t_1^* = t_1 - \frac{F_f}{2\eta F_m} (t_1 - t_0), \quad (17)$$

where μ is the friction coefficient. The friction state in the driving process is normally very complex and varies after every stroke. Especially, the surface roughness is changed higher after the first stroke than after the subsequent strokes. With Eq. 2 and 12, the bending angle θ is determined:

$$\theta = \frac{2V_{st}}{B} (t_1^* - t_0^*). \quad (18)$$

In addition, the deformation ϵ_2 denotes the necking at the flank edge reasonably (5).

3) *Springback and Reverse Bending*: If the force F_H falls below F_f , the bended L-sheet springs back. To calculate the springback angle θ_z , the similarity law of triangles is used on the flow curve [6] and

$$\theta_z = \frac{S_B L}{EB}. \quad (19)$$

Actually, the flank π_H has also a springback angle that is different from θ_z , so that the flank π_H should be bended back to find a new forming balance. Because the springback angles are even very small, the reverse bending is ignored here.

C. Evaluation

In this section, the model will be evaluated with standardized L-sheets, the force progression on stroke depths (Fig. 6(a)) and the stress-strain curve of the flat drawing (Fig. 6(b)). From the force progression, the force maximum

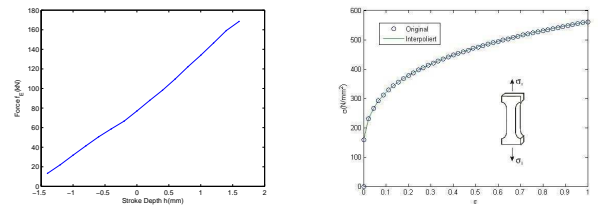


Fig. 6. Force progression on stroke depths (left); Stress-strain curve of flat drawing (right).

F_m in the time interval $[t_0, t_1]$ can be determined by the input stroke depth h . With the help of the stress-strain curve, the flow stress S_B is updated after every stroke, although the elastic, perfect plastic material model was used in the first phase. The flow stress S_H lies always on the 0.2% plastic limit $R_{p0.2}$ because of almost no changing of it. Additionally, the friction coefficient of the L-sheet is formulated as follows:

$$\mu = \begin{cases} \mu_0 & t = 0 \\ \mu_1 + \mu_2 \cdot Rand() & t > 0 \end{cases}. \quad (20)$$

A stochastic function $Rand()$ is employed to simulate the stochastic change of the surface roughness from one stroke to another stroke. Fig. 7 shows the results of the simulations

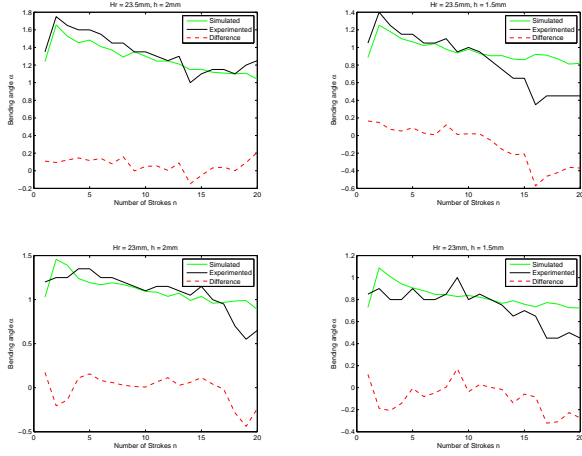


Fig. 7. The results of simulations and experiments (with parameters $B = 35mm$, $H = 50mm$, $T = 1.17mm$, $l_0 = 9mm$, $E = 210000N/mm^2$, $\nu=0.3$, $\xi = 0.85$, $\bar{H} = 23.5mm$, $\bar{h}=2mm$, $\mu_0=0.15$, $\mu_1=0.33$, $\mu_2 = 0.5$).

in comparison with the results of the experiments. It is to be seen that the most differences of the bending angles lie under $\pm 0.2^\circ$ (The material breaks already down after about 15 strokes).

Although many approximations were done in the modeling, this mathematical model has showed its relatively high accuracy with respect to the experiments. It describes the stretching process better than a FEM model and suitable for model based implementations.

III. MODEL PREDICTIVE CONTROL

A. MPC Strategy

At present, MPC as a popular control strategy is widely applied in process industry. MPC uses a model to predict outputs according to control inputs. In order to reach the set point y_s , a reference trajectory $y_r(k)$ is planned from the current output $y_o(k)$, namely,

$$y_r(k) = f_r(y_o(k), y_s). \quad (21)$$

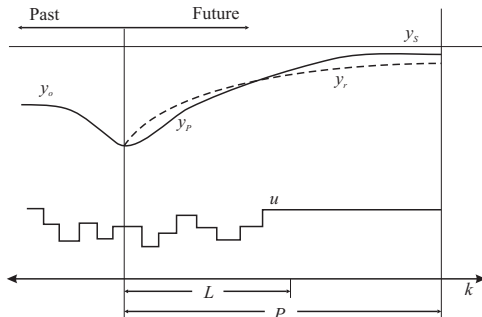


Fig. 8. Strategy of MPC.

The control input $u(k)$ must be carefully calculated. For it, an objective function $J(k)$ can be given. It should contain predictive errors in the predictive horizon P and terms about the control inputs. The general objective function is defined as follows:

$$J(k) = \|y_p(P) - y_r(P)\|_Q^2 + \sum_{k=1}^P \|y_p(k) - y_r(k)\|_Q^2 + \sum_{k=1}^L (\|u(k) - u_r(k)\|_R^2 + \|\Delta u(k)\|_S^2), \quad (22)$$

where $\|\bullet\|_Q^2$ is the weighted 2. norm with Q . With tuning the weights Q , R and S , each term can contribute to $J(k)$ comparably. The predictive horizon P and control horizon L can be identical. In practice, good results can be gained if P is greater than L . The both horizons can be chosen neither arbitrarily short nor arbitrarily long, because the prediction doesn't hold steady any more with a too short horizon and the long horizon slows down the prediction. Additionally, the model error $e(k) = y_o(k) - y_m(k)$ will be incorporated into the predictor $y_p(k+1) = y_m(k+1) + g \cdot e(k)$, where g is a weight.

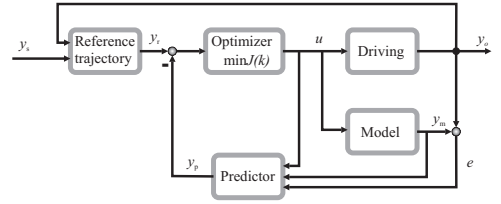


Fig. 9. Closed loop control of MPC

MPC control strategy can be used for a linear model and also a nonlinear model. The reference trajectory should be planned rationally due to output limitations. For optimizations analytical solutions should be firstly researched, because numerical methods can only supply approximated results. If there are no analytical solutions to be found out, the numerical methods are applied, which is profitable for a time discrete system. The optimal control input is renewed at each step, so that the effect of disturbance is held as little as possible.

B. Formulation of the Control Problem

In section II, the stretching process is modeled that it has elastic deformations in the both flanks π_B and π_H , plastic deformations in the flank π_B and in the both flanks as well as the springback. Hereby, only the totally plastic deformations are observed and formulated in the following:

Phase 1:

$$\theta^{P1} = \frac{2S_H l_0}{ET} \quad (23)$$

$$\theta_S(n - \frac{1}{2}) = \theta_S(n - 1) + \theta^{P1} \quad (24)$$

$$S_B(n - \frac{1}{2}) = S \left(\frac{B\theta_S(n - \frac{1}{2})}{l_0} \right)$$

$$F_f = \frac{1}{4}(2BS_B(n - \frac{1}{2}) + HTS_H/B)$$

Phase 2:

$$\theta^{P2} = \frac{2(A_{st} + h(n-1))}{B} \left(\frac{\pi}{2} - \phi \right) \cos \phi \quad (25)$$

$$\theta_S(n) = \theta_S(n - \frac{1}{2}) + \theta^{P2} \quad (26)$$

$$S_B(n) = S \left(\frac{B\theta_S(n)}{l_0} \right)$$

$$\phi = \frac{F_f}{\mu f(h(n-1))} \left(\frac{\pi}{2} - \gamma \right) + \gamma$$

$$\gamma = \arcsin \left(\frac{A_{st} + \Delta h(n-1)}{A_{st} + h(n-1)} \right)$$

Phase 3:

$$\theta^{P3}(n) = \theta^{P1}(n) + \theta^{P2}(n) - \frac{S_B(n)L}{EB} \quad (27)$$

In this mathematical model, the elastic forming is ignored and the output from the model is not null although the control input (stroke depth) is null, because the plastic deformations have already happened even only with null stroke depth but from certain reference positions. Actually, the control input stroke depth h has a limitation because of the machinery restraints. Hence, the output bending angle θ^{P3} has also a limit and it is stochastic because of the modelling of the friction coefficient (Eq. 20). To get the optimal stroke depth at every stroke, it is necessary to resolve the optimization problem according to the model and the objective function. Unfortunately, the model is nonlinear and it is also difficult to linearize it. The dynamic programming is a powerful method and can deal with the nonlinearity of the model and the limitations at the input/output.

C. Diskrete Dynamic Programming

In the phase of the optimization, the optimal control input is determined by minimizing the objective function $J(k)$:

$$u(k) = \mathbf{argmin}_{u(k)} J(k). \quad (28)$$

For a time discrete model, the discrete dynamic programming (DDP) is preferred [7].

1) *Principle*: For a dynamic optimization problem, the states $\mathbf{x}(0) = \mathbf{x}_0$ are transferred in a end condition $\mathbf{g}[\mathbf{x}(P), P] = 0$ with respect to the restrictions. In the figure 10, the principle of the optimality is clarified. There are two parts of the optimal state trajectory $x_{opt}(n)$. In the part 2 the states $x_{opt}(n_1)$ go onto the end condition along the optimal trajectory 2. If there could exist another optimal trajectory 3 with less costs, it is inconsistent with the indication of the optimal trajectory with minimal costs. The feature in the demonstrated optimality principle delivers a path to calculate the optimal trajectory numerically, so called "dynamic programming" (DP). A direct application is to solve combinatorial problems that indicate multi-stage determination problems. The determinations lie on each state from one stage to another stage, which is really connected with certain costs. The target of optimization is to find the shortest path with minimal costs from a initial stage to a final stage. In order to make numeric analysis of

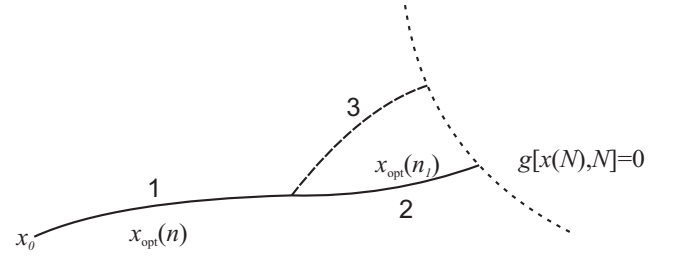


Fig. 10. Clarification of the optimality principle of the dynamic programming.

multi-stage procedures possible, the valid state field $\mathcal{X}(k)$ and the valid control field $\mathcal{U}[\mathbf{x}(k), k]$ are discretized in terms of appropriate grid points. The discretization interval $\Delta \mathbf{x}(k)$ and $\Delta \mathbf{u}(k)$ should be suitably chosen depending on formulated problems and desired solution accuraries. With the help of the discretization, the multi-stage procedure of DP is performed in the following. The use of a discrete control input $u(k)$ on one discrete state $x(k)$ goes into another state:

$$\mathbf{x}(k+1) = \mathbf{f}[x(k), u(k), k] \quad (29)$$

of the stage $k+1$. Actually, there are many transitions $u(k)$ at every state point $x(k)$. Consequently, optimal control value can result from direct comparisons of these transitions, so that the destination of the global minimum is guaranteed for the one-stage optimization. The multi-stage procedure leads then to a global minimum of the multi-stage optimization problem, because DP checks indirectly all the possible combinations of the transitions. This global minimum refers to the discrete problem and therefore shows an approximation of the solution of the initial control problem. But for the adequate small discrete intervals, the approximation can be arbitrarily created. The end condition $\mathbf{g}[\mathbf{x}(P)] = 0$ must be extended because of the discretization. A tolerance band $\pm \delta$ about the end condition is constructed by the definition of following set $\mathcal{G} = \{\mathbf{P} | \exists \beta : |\mathbf{x}(P) - \beta| \leq \delta, \mathbf{g}(\beta) = 0\}$. If $\mathbf{x}(P) \in \mathcal{G}$, the control goal could be achieved in terms of discrete problems.

2) *Creation of the Objective Function*: With respect to the equation (Eq. 22), the objective function of one-stage optimizations is specified for the stretching model as follows:

$$J(k) = Q(y_p(k) - y_r(k))^2 + R(u(k) - u_r(k))^2 + S\Delta u^2, \quad (30)$$

in which $u_r(k)$ is the reference control input (stroke depth), which can bring the sheets in a certain state with little distortion and anisotropic residual stresses. Furthermore, the control input can not change very huge in comparison to the last input, otherwise the material will break down earlier. The result from minimizing $J(k)$ is a optimal control law that is available in table form: for each grid point $x(k)$ the respective discrete control value $u(k)$ is known as the optimal transition to the next time point $k+1$. If an optimal control trajectory would derive from this control law, the cases can appear that the states $\mathbf{x}(k+1)$ either lie out of the valid state field $\mathcal{X}(k)$ or don't overlap any grid point of the stage

$k + 1$. In the first case, the transition will be disregarded. In contrast, an interpolation will be applied for the second case. The "nearest neighbour" interpolation is the simplest method, while the linear interpolation is also implemented

$$J_L(k) = \frac{(y(k) - y_1(k))}{(y_2(k) - y_1(k))} (J_2(k) - J_1(k)) + J_1(k), \quad (31)$$

where $J_1(k)$ and $J_2(k)$ are the costs resulted from $y_1(k)$ and $y_2(k)$ respectively. The current output $y(k)$ is then replaced by the nearest point ($y_1(k)$ or $y_2(k)$), so that no exploded calculations would come up.

3) *Calculation of the Control Input*: To determine the optimal control input, the path from the initial state point to the desired state point with minimal costs must be found out. For this purpose, the cost matrix C is firstly generated to clarify the transitions from one time point to another time point graphically, that is

$$\begin{pmatrix} \infty & c_{2,1} & c_{3,1} & \cdots & c_{i,1} & \infty & \cdots \\ c_{1,2} & \infty & \infty & \cdots & \infty & c_{i+1,2} & \cdots \\ c_{1,3} & \infty & \infty & \cdots & c_i & c_{i+1,3} & \cdots \\ \vdots & \vdots & \vdots & \ddots & \vdots & \vdots & \vdots \\ c_{1,i} & \infty & \infty & \cdots & \infty & c_{i+1,i} & \cdots \\ \infty & c_{2,i+1} & c_{3,i+1} & \cdots & c_{i,i+1} & \infty & \cdots \\ \vdots & \vdots & \vdots & \cdots & \vdots & \vdots & \ddots \end{pmatrix}, \quad (32)$$

where $c_{i,j} = c_{j,i}$. Furthermore, the Dijkstra's algorithmus [8] is employed to get the shortest path with the use of the cost matrix C .

D. Results

In this section, it is to test how highly the responsible parameters affect the control output. In the one-stage objective function $J(k)$, there are three available terms that are weighted with Q , R and S respectively. The results will show whether they really contribute something to the objective function. Normally, a fixed length of prediction horizon (PH) will be held. Against it, the results with a changing PH will be also gained. The "nearest neighbour" (NN) and linear (LN) interpolations (IP) will be tried to determine which method can render better results. The reference trajectory (RT) will be given, because there could exist a referencing sequence of strokes according to the material features. At last, the discretization interval will be scaled down to find the compromise between solution accuracies and calculation complexities. Because of the stochastic modelling of the friction coefficient, the mean $E(\theta^{P3} - \theta_r)$ and the variance $\sigma^2(\theta^{P3} - \theta_r)$ are chosen to present the results.

The length of the prediction horizon refers to an effective parameter. Normally, the MPC can only supply worse results with a short horizon. This doesn't denote that the better results could be gained with a longer horizon. From Tab. I, better control outputs result from $PH = 3$.

With the addition of the term $\Delta u^2(k)$ in the objective function, the control outputs can be advanced obviously. This

TABLE I
THE RESULTS FOR CONTROL OUTPUTS FROM DIFFERENT PARAMETERS.

| Q | S | R | PH | IP | RT | Δy | Δh | E | σ |
|-----|-----|-----|------|------|------|------------|------------|---------|----------|
| 1 | 0 | 0 | 1 | NN | 0 | 0.5 | 0.5 | 0.1786° | 0.0911° |
| 1 | 0 | 0 | 2 | NN | 0 | 0.5 | 0.5 | 0.1727° | 0.0477° |
| 1 | 0 | 0 | 3 | NN | 0 | 0.5 | 0.5 | 0.1475° | 0.0575° |
| 1 | 0 | 0 | 4 | NN | 0 | 0.5 | 0.5 | 0.1616° | 0.0217° |
| 1 | 0 | 0 | 5 | NN | 0 | 0.5 | 0.5 | 0.2033° | 0.0216° |
| 1 | 0 | 0 | 6 | NN | 0 | 0.5 | 0.5 | 0.2018° | 0.0415° |
| 1 | 1 | 0 | 3 | NN | 0 | 0.5 | 0.5 | 0.0851° | 0.0336° |
| 1 | 1 | 1 | 3 | NN | 0 | 0.5 | 0.5 | 0.0753° | 0.0146° |
| 1 | 1 | 1 | 3 | LN | 0 | 0.5 | 0.5 | 0.0231° | 0.0224° |
| 1 | 1 | 1 | 0 | LN | 0 | 0.5 | 0.5 | 0.0564° | 0.0549° |
| 1 | 1 | 1 | 3 | LN | 1 | 0.5 | 0.5 | 0.0240° | 0.0132° |
| 1 | 1 | 1 | 3 | LN | 0 | 0.1 | 0.1 | 0.2018° | 0.0920° |

term has the ability that no huge difference can appear between two consequent control inputs. In this regard, the material features are changed constantly and the supplementary measurement variations are largely reduced. Furthermore, the term $(u - u_r)^2$ is inserted in the objective function, because in the opinion of the forming technique the material features can be changed consequently with a suitable stroke depth. Hence, with a reference stroke depth, the control output is then a little advanced. Compared with the results from "nearest neighbour" interpolation, the linear interpolation has improved the results significantly, because the transition costs are calculated more accurately.

If the prediction length is decided by the valid prediction stages, the results are obviously worst ($PH = 0$). The reason for it is that the prediction horizon would be very short at the last strokes. In order to create a good functionality of the material, a reference trajectory of stroke depths can be provided ($RT = 1$). The quality of the control outputs stays almost unchanged. That is to say, if possible, such a reference trajectory should be given.

The discretization can play a role. Theoretically, more accurate control outputs can be obtained with smaller intervals. But in practice, it is to be seen that the worse outputs result from the smaller discretization intervals. The reason for it is that the transition costs varies hugely at a same transition compared with from the large intervals. Hereby, it presents a problem of the inductance coupling of the discretization intervals and the weights. The both parameters should be matched. Additionally, the complexity of DDP grows exponentially with the dimension of the state vector and control input vector. Altogether, the optimal parameters in this paper is $(Q, R, S, PH, IP, RT, \Delta y, \Delta h) = (1, 1, 1, 3, LN, 0, 0.5, 0.5)$ Due to the coarse discretization intervals and the relativ short horizon, the online computation is actually possible.

IV. CONCLUSIONS AND FUTURE WORKS

A. Conclusions

In the section II, the stretching process was modeled in the three phases that contain the hybrid deformations, the

material flow and the springback. In comparison with the results of experiments, the most differences of the bending angle are less than 0.2° , which is acceptable to be used in MPC. The key issue of MPC is the optimization problem. Because of the highly nonlinear discrete model, the powerful method DP was implemented to gain the optimal control input. It was also tested which parameters and how they affect the control outputs. The mean E and the variance σ^2 were used to choose the parameters because of the stochastic modeling of the friction coefficient μ . At this point, it should be denoted that DP can handle a stochastic process very well.

B. Future Works

In this paper, a reasonable combination of the parameters was found out. In the future, the parameters will be tuned finely to identify the appropriate domains and their combinations. This could be achieved through an advanced optimization using an objective function that has terms the mean E and the variance σ^2 of the errors, for example $E \cdot \sigma^2$. This denotes also the learning process, in which E and σ^2 are calculated from the past inputs and outputs. Furthermore, a hybrid control strategy can practically gain more advantages. In the future, MPC will be combined with another control strategy (e.g. Iterative Learning Control). The online experiments will be done in the next works.

REFERENCES

- [1] H. Hoffmann and R. Petry, "Mass Customization of Sheet Metal Parts by Numerically Controlled Driving", *SheMet05 - International Conference on Sheet Metal*, Erlangen, 2005.
- [2] M. Tseng and F.T. Piller, *The Customer Centric Enterprise. Advances in Mass Customization and Personalization*, Springer, New York, Berlin 2003.
- [3] Z. Yang, M. Markert, D. Scherer, M. Golle, S. Weber, H. Hoffmann, B. Lohmann and T.C. Lüth, "Driving Using A Cognitive Method For Production of Customized Sheet Metal Parts", *IFAC Workshop on Manufacturing Modelling, Management and Control*, Budapest, Hungary, November 2007.
- [4] Z. Yang, M. Markert, D. Scherer, M. Golle, S. Weber, H. Hoffmann, B. Lohmann and T.C. Lüth, "A Human-Machine interactive Driving System", *IEEE International Conference on Distributed Human-Machine Systems*, Athens, Greece, March 2008.
- [5] E.F. Camacho and C. Bordons, *Model Predictive Control*, Springer, London, 2004.
- [6] Z. Yang and B. Lohmann, *Modellierung des inkrementellen Verformungsprozesses des L-Blechtes*, Internal Report, April 2008.
- [7] M. Papageorgiou and O. von Stryk *Optimierung*, Springer, Berlin, 2006.
- [8] E.W. Dijkstra, A note on two problems in connexion with graphs, *In: Numerische Mathematik.*, vol. 1, 1959, pp 269-271.